JOURNAL OF QUATERNARY SCIENCE (2014) **29**(6) 531–546 ISSN 0267-8179. DOI: 10.1002/jqs.2723

Re-evaluation of the Roseau Tuff eruptive sequence and other Ignimbrites in Dominica, Lesser Antilles

TRACY M. HOWE,[1]* JAN M. LINDSAY,[1] PHIL SHANE,[1] AXEL K. SCHMITT[2] and DANIEL F. STOCKLI[3]
[1]School of Environment, University of Auckland, Private Bag 92019, Auckland, New Zealand
[2]Department of Earth, Planetary and Space Sciences, University of California, Los Angeles, CA, USA
[3]Department of Geological Sciences, University of Texas at Austin, TX, USA

Received 16 March 2014; Revised 12 May 2014; Accepted 18 May 2014

ABSTRACT: The island of Dominica hosts several ignimbrites, including the Roseau Tuff, thought to represent the largest eruption in the Caribbean in the past 200 000 years. The volcanic stratigraphy of the island is poorly understood due to limited outcrops and a paucity of geochemical and geochronological data. The discovery of a new fully accessible exposure of three ignimbrites intercalated with paleosols provides an opportunity to re-evaluate the current stratigraphic framework of ignimbrite-forming eruptions on the island. Whole-rock analyses of pumice clasts from Dominica ignimbrites are andesitic (61–66% SiO_2) and in most cases are geochemically indistinguishable. Ignimbrites in the north of the island have less evolved glass compositions (73–75% SiO_2) and more mafic orthopyroxene compositions (En > 56) than their southern counterparts (75–78% SiO_2; En < 56). Pumice clasts from ignimbrites in southern Dominica have indistinguishable groundmass glass and mineral chemistry, making correlation of these deposits difficult. New (U–Th)/He eruption ages for the southern ignimbrites indicate that at least six separate explosive eruptions occurred between 24 and 61 ka. The non-unique geochemistry of these deposits, together with the new (U−Th)/He ages, suggests that the large volume inferred for the Roseau Tuff eruption may actually be a composite of six smaller, geochemically homogeneous eruptions.

KEYWORDS: correlation; ignimbrites; Lesser Antilles; Roseau tuff; tephra; (U−Th)/He geochronology.

Introduction

Stratigraphic correlation of volcanic deposits plays a critical role in evaluating the frequency and magnitude of eruptions. However, in regions with hilly terrain, high rainfall and fast weathering rates, the patchy preservation of loose pyroclastic deposits limits field-based reconstructions, especially where there is a paucity of materials for radiometric dating. In such environments, the establishment of a reliable volcanic stratigraphy is greatly enhanced by petrographic and geochemical fingerprinting of deposits of known source and/or age (Westgate and Gorton, 1981; Hildreth and Mahood, 1985; Sarna-Wojcicki, 2000; Shane and Smith, 2000). This is especially true for island arc regions where much of the volcanic material is preserved offshore (Sigurdsson and Carey, 1981). Lithological characteristics alone are often insufficient to yield reliable onshore to offshore correlations (Sarna-Wojcicki, 2000), and thus correlation is augmented by geochemical data. Geochemical characteristics of deposits, however, are commonly non-unique (Brendryen *et al.*, 2010; Lowe, 2011). Radiometric dating of late Quaternary volcanic deposits can yield robust correlations, but traditionally this has been limited to samples that contain non-weathered carbonaceous material (^{14}C geochronology) or high-K mineral phases, such as sanidine (K−Ar and ^{40}Ar–^{39}Ar geochronology). In many situations such materials are absent or altered. The development of (U−Th)/He geochronology has provided a new approach for dating young volcanic deposits (Farley, 2002; Schmitt *et al.*, 2010a, b; Danišík *et al.*, 2012). Limited only by the presence of dateable accessory phases, such as zircon and apatite, (U−Th)/He geochronology can be used to fill chronological gaps in regions where other dating methods are not feasible.

Located in the centre of the Lesser Antilles arc (Fig. 1A), the island of Dominica exemplifies many difficulties associated with volcanic deposit correlation in tropical environments. Three major silicic ignimbrites dated between 30 and 45k cal a BP by ^{14}C geochronology have been identified on the island (Sigurdsson, 1972; Sparks *et al.*, 1980; Lindsay *et al.*, 2003; Smith *et al.*, 2013). Due to poor exposure, mineralogical and compositional homogeneity, and reworking of deposits by volcano flank-collapse, their stratigraphic relationships are difficult to decipher. Because most of the deposits lack comprehensive geochemical and geochronological characterization, the volcanic stratigraphy of Dominica is currently poorly constrained. Carey and Sigurdsson (1980) correlated pyroclastic flow and fall materials in 26 deep sea cores from the Atlantic Ocean and Caribbean Sea to a single pyroclastic flow on the island, referred to as the Roseau Tuff (Fig. 1; Sigurdsson, 1972). Based on glass and mineral chemistry, they proposed that >55 km^3 of unconsolidated off-shore tephra deposits, consisting of ~25 km^3 of fall out layers and another ~30 km^3 of pyroclastic flow material, were the result of a single eruption. The Roseau Tuff is thus considered the largest Caribbean eruption in the past 200 000 years. Despite its voluminous nature, however, <3 km^3 (unconsolidated) of volcanic material is thought to be preserved on the island (Carey and Sigurdsson, 1980). In a more recent study by Smith *et al.* (2013), it was suggested that the submarine deposits regarded by previous authors as being entirely related to the Roseau Tuff probably represent a composite of material from multiple Plinian eruptions from across the island. Smith *et al.* (2013) further state that the Roseau Tuff eruption itself can be subdivided based on ^{14}C ages into seven separate eruptive episodes, which all display overlapping whole rock compositions.

In this study, we focus on Dominica's subaerial pyroclastic flow deposits, with the specific aim of fingerprinting the pumiceous pyroclastic flow deposits using whole rock, mineral and glass chemistry of pumices. We also attempt to improve the age control of major pyroclastic units using both zircon and apatite (U–Th)/He geochronology. Based on these new data, we discuss the chronological and stratigraphic framework of late Quaternary pyroclastic eruptions on

*Correspondence: Tracy M. Howe, as above.
E-mail: t.howe@auckland.ac.nz

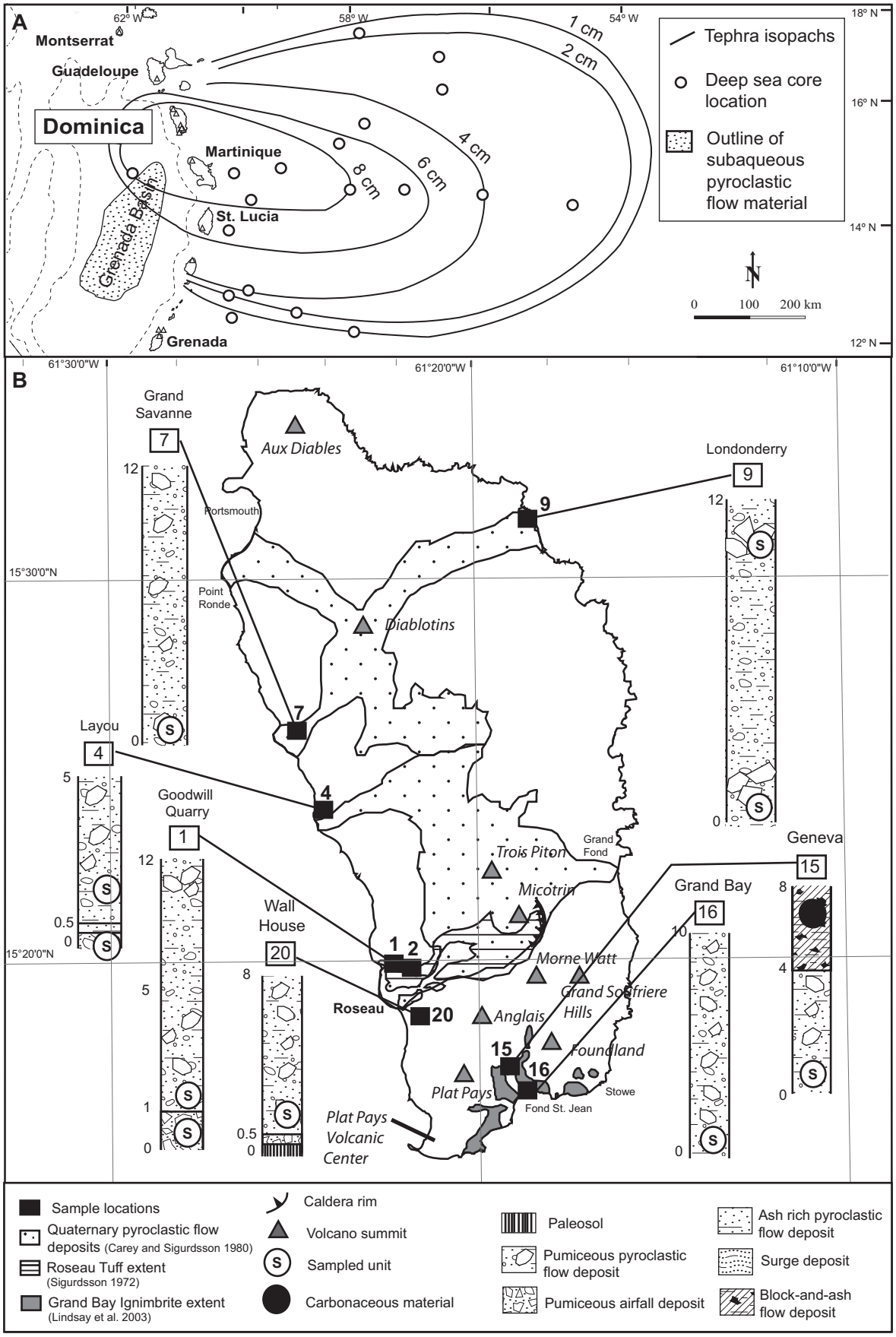

Figure 1. (A) Map of the Lesser Antilles arc, including core locations and tephra isopachs used by Carey and Sigurdsson (1980) to determine the extent and volume of the Roseau Tuff. (B) Sketch map of Dominica showing sample locations and the previously mapped extent of major ignimbrite formations. Place names and volcanoes (triangles) are shown for reference. Generalized stratigraphic logs of key outcrops are also shown. Numbers located on the side of each stratigraphic log indicate the height in meters. For the stratigraphic log of Location 2, see Fig. 2.

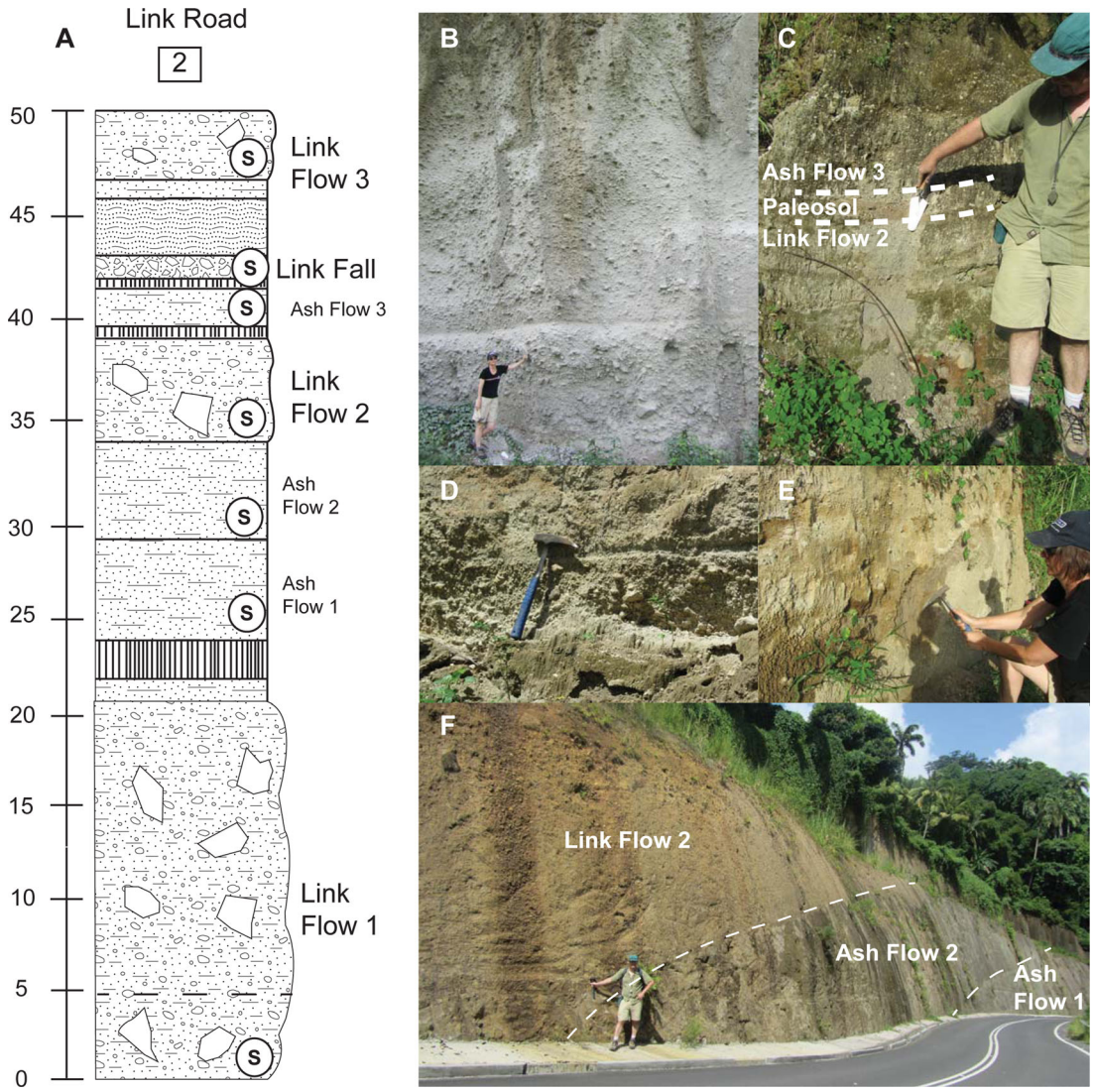

Figure 2. (A) Stratigraphic log of the Link Road deposits (Location 2; Fig. 1). See Fig. 1 for legend. Scale on the side indicates the height in meters. Dashed line at ~5 m indicates possible flow break. (B–F) Photographs of Link Road deposits: (B) Link Flow 1; (C) the contacts between Link Flow 2, the overlying paleosol and ash flow; (D) a close up of the Link Fall deposit; (E) the Link Flow 3 deposit; and (F) an overview of a large section of the Link Road deposit. White lines are used to indicate contacts between units. This figure is available in colour online at wileyonlinelibrary.com.

Dominica, especially with regard to the Roseau Tuff eruption. We also examine implications for tephrostratigraphy in the Lesser Antilles, specifically in relation to the correlation of offshore material to onshore deposits.

Geological Setting

The Lesser Antilles island arc consists of 11 volcanic islands and marks the westward subduction of the North American and South American plates beneath the Caribbean plate (Fig. 1A; Lindsay *et al.*, 2005). The arc is physically segmented with the northern segment trending at 330° and the southern segment trending at 020° (Wadge and Shepherd, 1984). Situated at the center of the arc curvature between Martinique and Guadeloupe, Dominica is the largest and most mountainous island in the arc (Wadge and Shepherd, 1984). The island has eight potentially active volcanic centers, including two possible calderas (Demange *et al.*, 1985; Lindsay *et al.*, 2005). Although the topography of Dominica is dominated by volcanic domes and their associated deposits, pumiceous pyroclastic flow sheets outcrop across the island, providing evidence of ignimbrite-forming eruptions. Three major pyroclastic flow deposits have been mapped: the Roseau Tuff (Sigurdsson, 1972), the Grand Bay Ignimbrite (Lindsay *et al.*, 2003) and the Grand Savanne Ignimbrite (Sparks *et al.*, 1980) (Table 1, Fig. 1). We refer to these deposits as ignimbrites and use the term to refer to pumiceous pyroclastic flow deposits. Although Smith *et al.* (2013) identified multiple pyroclastic outcrops associated with each of the three main ignimbrites, limited outcrop access and exposure constrained our ability to sample every pyroclastic flow deposit on the island. Therefore, our interpretations are based on the outcrops accessible at the time of our fieldwork only and we make no assumptions about unsampled outcrops. We did not sample pyroclastic flow deposits at Point Ronde, Grand Fond and Fond. St. Jean (Fig. 1). A detailed overview of the main three ignimbrites is discussed below.

Roseau Tuff

The Roseau Tuff is a partly welded ignimbrite that outcrops throughout the Roseau Valley (Fig. 1). Originally mapped by Sigurdsson (1972) as a series of andesitic pyroclastic flow

Table 1. Locations and descriptions of outcrops.

Field stop	Outcrop name	GPS location	Location description	Outcrop description	Previous correlations	Mineralogy
1	Goodwill	15°18.506N, 61°23.067W	Road outcrop inside Goodwill Quarry	Pumiceous fall deposit overlain by a 5-m pumiceous pyroclastic flow	Roseau Tuff[1]	pl >>opx > cpx
2	Link Road	15°18.256N, 61°22.465W	Road outcrop along Santa Romet Road	Three pumiceous pyroclastic flow deposits interspersed with finer ash-grade flows, paleosols, and a single pumiceous fall deposit (Fig. 2)		pl >>cpx > opx > amp
4	*Layou	15°23.859N, 61°25.607W	Road outcrop just north of the Layou River	Pumiceous fall deposit overlain by a thin (~5 cm) layer of white ash and a 4-m pyroclastic flow deposit	Roseau Tuff[2] Layou Ignimbrite[3]	pl >>opx > amp
15	*Geneva	15°14.951N, 61°19.020W	Geneva Estate Quarry	4-m pumiceous pyroclastic flow overlain by an andesitic block and ash flow deposit	Grand Bay Ignimbrite[4] Roseau Tuff[3]	pl >>cpx > opx
16	*Grand Bay	15°14.553N, 61°18.701W	Grand Bay beach–type locality	10-m pumiceous pyroclastic flow deposit.	Grand Bay Ignimbrite[4] Roseau Tuff[3]	pl >>opx > cpx
20	*Wall House	15°16.976N, 61°22.663W	Wall House Quarry, south of Roseau	Pumiceous fallout deposit overlain by a lithic-rich, 5–6-m pyroclastic flow deposit	Grand Bay Ignimbrite[4] Roseau Tuff[3]	pl >>opx > cpx
7	Grande Savanne	15°26.349N, 61°26.379W	Road outcrop located 500 m north of Salisbury	Pumiceous pyroclastic flow deposit overlying a series of surge deposits	Grande Savanne Ignimbrite[5]	pl >>opx > cpx
9	Londonderry	15°33.614N, 61°17.832W	Beach outcrop just north of Londonderry river	15-m-thick pyroclastic flow deposit with two clear pumice accumulation zones	Wesley Flow[3]	pl >>opx > cpx

Field stop numbers given in the first column correspond to sample locations shown on Fig. 1. The mineralogy of each unit is also shown. *Deposits that have been varyingly correlated by previous authors, see column 5 for past correlations. Superscripts indicate references as follows: 1 = Sigurdsson (1972); 2 = Whitham (1989); 3 = Smith *et al.* (2013); 4 = Lindsay *et al.* (2003); 5 = Sparks *et al.* (1980).

deposits ranging in age from 31 to 46k cal a BP (Table 2), the unwelded sequence consists of four major pyroclastic flow units (Units I, II, III and IV) with 'weathered horizons' between them. Mapping by Demange *et al.* (1985) confirmed the presence of paleosols between these units. Although no direct contacts have been located, these units are thought to overlie the welded Roseau Tuff, a large welded pyroclastic deposit that outcrops at higher elevations and has been

Table 2. Previous ages of pyroclastic flow deposits.

Ignimbrite and Deposit type	Location	^{14}C age ± 1 SD (a BP)	Calibrated ^{14}C age ± 1 SD (cal a BP)	Reference
Roseau Tuff				
Ignimbrite	Micotrin Ring Road	26 380 ± 190	29 234 ± 362	1
Ignimbrite	Grand Fond	27 600 ± 600	30 364 ± 522	2
Ignimbrite	Goodwill quarry (Unit II)	28 400 ± 900	31 000 ± 800	3
Fallout pumice	Goodwill Quarry (topmost airfall unit)	29 000 ± 4200	31 800 ± 4200	2
Ignimbrite	Goodwill Quarry (pyroclastic unit, 7 m above base)	>33 200	>33 200	2
Ignimbrite	Goodwill Quarry (Unit I)	>34 000	>34 000	3
Fallout pumice	Goodwill Quarry	35 000 ± 2200	37 200 ± 2300	4
Ignimbrite	Goodwill Quarry (Unit I)	>46 000	>46 000	3
Layou				
Ignimbrite	Layou Valley	>40 000	>40 000	4
Grand Bay				
Distal facies	Near Stowe	>27 200	>27 200	5
Distal facies	Wall House Quarry	30 270 ± 200	32 482 ± 169	1
Distal facies	Fond St. Jean	>36 800	>36 800	5
Ignimbrite	Wall House Quarry	38 600 ± 400	41 100 ± 600	6
Distal facies	Fond St. Jean	38 890 ± 600	41 246 ± 659	1
Grand Savanne				
Pumiceous surge	Grand Savanne Beach	>22 200	>22 200	7

References are as follows: 1 = Lindsay *et al.* (2005); 2 = Carey and Sigurdsson (1980); 3 = Sigurdsson (1972); 4 = Wadge (1989); 5 = Sigurdsson and Carey (1991); 6 = Lindsay *et al.* (2003); 7 = Sparks *et al.* (1980). ^{14}C ages were calibrated using CalPal Online (ver. 1.5). Note: all ages listed in this table were obtained on charcoal material.

grouped by previous authors as part of Unit I (Demange *et al.*, 1985; Smith *et al.*, 2013). Using glass chemistry, Carey and Sigurdsson (1980) correlated deep-sea tephra layers (Fig. 1A) to the unwelded exposure of the Roseau Tuff at Goodwill Quarry, the type locality of the deposit (Fig. 1B). Using these correlations and isopachs based on tephra thickness in the cores, they estimated the total tephra volume of the Unit I eruption as 58 km^3 (unconsolidated) and suggested that the on-land portion of the ignimbrite represents only 5% of the total deposit. In contrast, Smith *et al.* (2013) suggested that this estimate actually represents a composite of multiple eruptions from different centers across the island. Smith *et al.* (2013) further suggested that the Roseau Tuff can be divided into seven separate eruptive episodes based on ^{14}C ages, which span a considerable time gap (>16 ka, from 30 to >46k cal a BP) with many ages not overlapping in uncertainty. The source of the Roseau Tuff has also been a matter of debate. Sigurdsson (1972) suggested Micotrin volcano, a large dome complex located in the central highlands of Dominica (Fig. 1), as the source of the eruptive sequence. Carey and Sigurdsson (1980), however, noted that the large calculated volume of the basal Roseau Tuff eruption indicated the existence of a possible caldera. Field mapping by Demange *et al.* (1985) proposed a caldera at Wotten Waven, which is now mostly buried beneath Micotrin volcano. Subsequent workers have considered Wotten Waven to be the likely source of the Roseau Tuff eruption (Demange *et al.*, 1985; Lindsay *et al.*, 2005; Smith *et al.*, 2013). Although Whitham (1989) correlated pyroclastic flow deposits in the adjacent Layou Valley (Fig. 1) to the Roseau Tuff, Smith *et al.* (2013) suggested that these deposits are actually sourced from Trois Piton volcano (Fig. 1).

Grand Bay Ignimbrite

The Grand Bay Ignimbrite is a laterally extensive andesitic pumiceous pyroclastic flow deposit that outcrops along the southern coast of Dominica (Lindsay *et al.*, 2003). Originally mapped at Grand Bay Beach (Location 16; Fig. 1), the deposit was correlated by Lindsay *et al.* (2003) to pyroclastic flow deposits at the Geneva and Wall House quarries (Location 15; Location 20; Fig. 1). ^{14}C ages on buried plant material taken from distal outcrops correlated to this ignimbrite at Stowe, Fond St. Jean and the Wall House quarry indicate eruption ages of 27–42k cal a BP (Table 2). However, field mapping by Smith *et al.* (2013) indicates that these distal outcrops may not be lateral equivalents of the Grand Bay Ignimbrite. Therefore, the age of the Grand Bay Ignimbrite is unconstrained. Lindsay *et al.* (2003) ruled out correlation of the Grand Bay Ignimbrite with the Roseau Tuff based on mineralogical and topographic constraints. Originally, the Plat Pays Volcanic Center, a large volcanic complex located on the south-western side of the island, was proposed as the source of the Grand Bay Ignimbrite (Lindsay *et al.*, 2003), but more recent work implicated Wotten Waven caldera as a possible source (Lindsay *et al.*, 2005; Smith *et al.*, 2013). Although Smith *et al.* (2013) suggested that the Grand Bay and Wall House deposits are part of the Roseau Sequence based on overlapping whole rock geochemistry, the relationship between the Grand Bay Ignimbrite and the Roseau Tuff remains unclear.

Grand Savanne Ignimbrite

A prominent submarine fan on the north-western side of the island marks the location of the Grand Savanne Ignimbrite, another thick pyroclastic flow sequence (Location 7; Fig. 1; Sparks *et al.*, 1980). Originally mapped by Sparks *et al.* (1980), the ignimbrite was thought to consist of two crystal-rich ash flow units with a distinct lack of pumice clasts. Detailed mapping by Smith *et al.* (2013), however, separated this deposit into a lower sequence consisting of three separate ignimbrite units and an upper sequence dominated by pumiceous surge deposits. At low elevations, the ignimbrite is commonly welded and overlies a block-and-ash flow deposit correlated to Diablotins, a large stratovolcano that dominates north-central Dominica (Fig. 1; Smith *et al.*, 2013). Organic material from a pumiceous surge deposit within the upper sequence indicates an age of >22 000 years (Table 2; Sparks *et al.*, 1980). Subsequent field studies showed a lack of paleosols between the two units, suggesting that both units formed during a continuous eruption (Smith *et al.*, 2013). Pyroclastic flow deposits at Londonderry beach on the north-eastern side of the island (Sparks *et al.*, 1980) were recently re-mapped as the Wesley pyroclastic flow fan (Smith *et al.*, 2013; Location 9; Fig. 1). The Wesley flow fan spans 4.6 km of Dominica's north-eastern coast and can be subdivided into two eruptive units separated by a thin paleosol (Smith *et al.*, 2013). Although the Wesley flow fan is sourced from Diablotins volcano based on topographical constraints, its eruption age is unknown and its relationship to the Grand Savanne Ignimbrite remains unclear (Smith *et al.*, 2013).

Methods

Sampling

Ten pyroclastic flow deposits were sampled (Fig. 1; Table 1). At locations where pyroclastic flow deposits overlie pumiceous fall deposits with no intervening paleosol, the fall deposit was also sampled. For pumiceous pyroclastic flow deposits, four to five pumice clasts from each pyroclastic unit at each outcrop were collected and individually analysed for whole rock major and trace elements. For pumiceous fall deposits, about five small pumice clasts were collected. No matrix material from pumiceous flow or fall deposits was collected. One to two pumice clasts from each unit were crushed for zircon separation and mineral and groundmass glass shard picking. For the three non-pumiceous ashy pyroclastic flow deposits (i.e. Ash Flow 1, Ash Flow 2 and Ash Flow 3 (Fig. 2)), only unconsolidated matrix material was available for sampling. Because ash samples do not necessarily represent magmatic compositions due to physical fractionation during transport and deposition, no major and trace element analyses were done on these units. Separated glass shards and magnetites from the ashy pyroclastic flows were analysed by electron microprobe.

A total of 40 pumice clasts were geochemically analysed. Pumice clasts from six units were selected for age dating by (U−Th)/He methods. Pumice clasts from the Grand Bay Ignimbrite were dated by apatite only, while pumice clasts from Link Flow 1 and Link Flow 3 were dated by zircon only. Pumice clasts from Layou, Londonderry and the Goodwill Quarry were dated by both zircon and apatite. Mineral chemistry was undertaken on 1–2 pumices from each unit studied.

Whole rock major and trace elements

Whole rock major elements and V, Zr and Zn were determined on 40 pumice clasts from the 10 locations by using a Siemens SRS3000 sequential X-ray spectrometer at the University of Auckland. Fused disk preparation was completed following the method of Norrish and Chappell (1977). Accuracy and precision of major and trace elements were determined using the USGS BCR-2 and AGV-2 standard

powders. Major elements achieve an accuracy of <3.5% with a precision of <2% (1 standard deviation; SD) (see supporting Table S2). Trace elements were determined by ablating fused X-ray fluorescence (XRF) disks with the Excimer LPX 120 laser and attached quadropole ICP-MS (Agilent 770 CS) at the Australian National University, Canberra (ANU). Ablation was done under an Ar–He stratified environment (30% He, 70% Ar) with a scan speed of 20 μm s^{-1} and a spot size of ~100 μm. With the exception of V, Zr and Zn all trace elements have <10% accuracy with a precision of <5% (Table S2). Values for V, Zr and Zn were taken from the XRF dataset.

Mineral and glass chemistry

Major element analyses of groundmass glass shards and individual crystals from pumice clasts were carried out using a JEOL JXA-850A electron microprobe at the University of Auckland. The accelerating voltage was 15 kV, and the beam current was 0.8 nA. All analyses were done using a count time of 100 s. An ~2-μm focused beam was used for mineral analyses, while an ~10-μm defocused beam was used for glass analyses. All glass analyses were normalized to 100% water free to account for variable hydration. Samples were prepared following the methodology of Froggatt and Gosson (1982). Accuracy and precision were determined by repeat analysis of ASTIMEX glass and mineral standards. Typical deviations of replicate glass analyses relative to the reference values are SiO_2 (<±0.13%), TiO_2 (<±7.5%), Al_2O_3 (<±0.90%), FeO (<±3.2%), MnO (<±25%), MgO (<±6.5%), CaO (<±8.6%), Na_2O (<±1.2%), K_2O (<±4.4%) and Cl (<±10%). All major oxides in minerals have errors <5% except at low abundances (i.e. <0.1 wt%) where the error increases to >25%. For individual pumice clasts, 10–15 pyroxene crystals, 10–20 titanomagnetite crystals, and at least five ilmenite crystals were analysed. A minimum of five plagioclase crystals per pumice clast were selected for profiling. For clasts containing amphibole, a minimum of five amphibole crystals were selected for analysis. For each pumice clast, 5–10 groundmass glass analyses were collected. For the three ashy pyroclastic flow deposits, microprobe analyses were done on individual glass shards and magnetite extracted from the matrix.

(U–Th)/He geochronology

Zircon separation was completed following the protocols detailed in Schmitt *et al.* (2006), and rim U–Th and U–Pb isotopic analyses of unpolished crystals were performed using the UCLA CAMECA ims 1270 following Schmitt *et al.* (2010b). Zircons >30 μm were embedded in indium mounts; those <30 μm were embedded in aluminum. Analyses were performed using a ~40–100-nA mass-filtered $^{16}O^-$ primary ion beam focused into a 25 × 30-μm spot. Secondary ions were accelerated using a voltage of 10 keV with an energy bandpass of 50 eV and a mass resolution of ~5000. Analyses were done in both mono- and multi-collector mode. Accuracy was monitored by intermittent analysis of zircon equilibrium standard AS3 (1099.1 Ma; Paces and Miller, 1993). For the mono-collection session, the AS3 (^{230}Th)/(^{238}U) weighted mean value was 0.989 ± 0.13 (mean square weighted deviation (MSWD) = 4.5; $n = 7$) and for multi-collection analyses, it was 0.991 ± 0.005 (MSWD = 1.6; $n = 23$). Zircon crystallization ages were calculated using the two-point isochron method and the whole rock ($^{230}Th/^{232}Th$) and ($^{238}Th/^{232}Th$) ratios determined from U-series analysis.

For combined U–Th and (U–Th)/He analysis, single grains were extracted from the U–Th mounts, photographed and packed into platinum tubes (Schmitt *et al.*, 2006). Helium degassing and isotope dilution ICP-MS analysis of U and Th were performed at the University of Texas, Austin, following methods described in Biswas *et al.* (2007) (U–Th)/He zircon ages from the Fish Canyon Tuff standard average 27.8 ± 0.8 (relative SD% 7.5; $n = 162$). Based on the reproducibility of such standard data and taking into account the low uranium concentration of Dominican zircons, we assigned 16% uncertainty to the uncorrected (U–Th)/He ages. Because of uranium series disequilibrium, uncorrected ages often underestimate the eruption age (Farley *et al.*, 2002). Disequilibrium corrections were applied using the UCLA MCHeCalc program described in Schmitt *et al.* (2010b). We report the individual disequilibrium-corrected ages, the full disequilibrium ages and a Gaussian fit for the average eruption age. Q values were used to quantify the goodness-of-fit as described by Press *et al.* (1992). The average age was considered acceptable for $Q > 0.001$ and $n > 4$, where n is the number of aliquots included in the sample set. Average ages are presented with 1SD errors. Because all U–Th analyses on Dominican zircons are rim analyses, crystallization ages here represent the lower limit of the bulk crystallization age. If crystals are highly zoned in age, the assumption of the rim age representing the bulk age will lead to an overcorrected eruption age (i.e. the age will be too old). Low Q values and eruption ages greater than crystallization ages indicated (U–Th)/He age overcorrection. In these cases, we assumed secular equilibrium for the crystal interior following Schmitt *et al.* (2010a). Full disequilibrium ages were calculated following the formulas in Farley *et al.* (2002); these ages assume the zircon crystallized at the time of eruption and represent the maximum corrected age of each aliquot.

Apatites were separated following the methods detailed in Schmitt *et al.* (2006). Inclusion-free, euhedral apatites 60–150 μm in size were selected for analysis. For each aliquot, 5–7 grains were measured, photographed and packed into a platinum tube. Helium degassing and isotope dilution ICP-MS analysis of U, Th and Sm were performed at the University of Texas, Austin. Aliquot ages were calculated following the methodologies in Farley (2000). Full disequilibrium ages were calculated following Farley *et al.* (2002), but had a negligible effect on the calculated age and so are not presented. Final ages for each sample were determined by taking the mean of all aliquot ages.

Results

The locations and schematic stratigraphic logs of studied deposits are shown in Fig. 1. During fieldwork in 2011, a new outcrop was examined within the confines of the Roseau Valley along the Santa Romet Link Road (Location 2; Figs 1 and 2). Referred to as the Link Road outcrop, this sequence consists of three pumiceous pyroclastic flow deposits interspersed with three finer ash-grade flow deposits, paleosols and a single pumiceous fall deposit (Fig. 2). The coarse pumiceous flow deposits are labeled Link Flow 1, Link Flow 2 and Link Flow 3, while the finer grained ash flow deposits are labeled Ash Flow 1, Ash Flow 2, and Ash Flow 3. The pumiceous fall deposit, labeled Link Fall, occurs between Link Flows 2 and 3. The presence of soil horizons between these flows indicates time breaks between their depositions (Fig. 2).

Although many of the deposits investigated in our study were previously correlated to one of the three major ignimbrite-forming eruptions discussed above, given the contradictory correlations in previous work, we reassess the stratigraphy without regard to previous correlations. Deposits

are thus referred to by their outcrop names. Except in cases where soil horizons clearly delineate units within a given outcrop, related pumiceous flows and falls at individual outcrops are grouped together for simplicity.

Whole rock geochemistry

Analysed pumice clasts from all the pyroclastic flow deposits are medium-K, calcalkaline andesites to dacites (57–66 wt% SiO_2) (Fig. 3A, E; Table S2). Supporting Table S1 includes the full suite of whole rock, glass and mineral chemistry data used in this project. Most pumice clasts contain between 61 and 66 wt% SiO_2 with those from Layou being the most evolved and those from Grand Savanne being the least evolved. In general, pumice compositions from the Grand Bay, Geneva and Wall House outcrops fall within the Goodwill Quarry field (Fig. 3A–C). However, these samples are distinguished by elevated Nb compared with the Goodwill Quarry samples (Fig. 3D). Pumices from the Layou, Grand Savanne and Londonderry deposits are chemically distinct (Fig. 3A–D). The Londonderry samples have higher TiO_2, Al_2O_3, FeO and K_2O than the Goodwill Quarry samples, whereas the Grand Savanne samples are chemically heterogeneous and range from 62 to 64.5 wt% SiO_2 with variable amounts of TiO_2, FeO, MgO and CaO. Although chemical analyses of pumices from all three of the coarse-grained Link Road units plot within the Goodwill Quarry field, some clasts are somewhat geochemically distinct (Fig. 3E–H). The Link Fall deposit also plots within or very close to the Goodwill compositional field. Rare earth element (REE) plots show that the southern pyroclastic flow deposits (including the Goodwill Quarry, Link Road, Grand Bay, Geneva and Wall House outcrops) have a restricted range in composition (Fig. 4A). Layou has slightly lower concentrations of heavy REEs (Fig. 4B), while Londonderry has higher concentrations (Fig. 4C). The Grand Savanne unit shows a large range in REE compositions, including some higher concentrations than other deposits (Fig. 4D).

Glass major element compositions

Groundmass glasses from all units are rhyolitic, with 73–78 wt% SiO_2 (Fig. 5A; see Table S3). Glass analyses from Goodwill Quarry pumices display a restricted range in SiO_2 content (~75–77 wt%). Glass analyses from the Geneva and Wall House pumices fall within the Goodwill Quarry field, whereas those from Grand Bay pumices have slightly higher silica contents (Fig. 5A). Grand Savanne and Londonderry pumices are characterized by lower SiO_2 contents than those of the other ignimbrites (Fig. 5A). Although the average Goodwill Quarry glass analysis of Carey and Sigurdsson (1980) overlaps with our data for some elements, there are significant differences in the CaO, Al_2O_3 and K_2O values (Fig. 5A, B). These differences could reflect differences in analytical conditions.

The glass chemistry for the Link Road pumices shows some clear distinctions between eruptive units (Fig. 5C, D). Although all Link Road deposits show significant overlap with the Goodwill Quarry field (Fig. 5C, D), Link Flow 1 has higher K_2O (Fig. 5C) and lower FeO (Fig. 5D). Ash Flow 3 also falls within the Goodwill field and overlaps geochemically with Link Flow 2 and Link Fall. Ash Flows 1 and 2 are characterized by microlites in the glass preventing fingerprinting.

Petrography and mineral chemistry

Pumice clasts from all outcrops share a similar mineralogical assemblage, consisting of plagioclase (15–24%), Fe–Ti oxides (0–4%), clinopyroxene (0–3%) and orthopyroxene (0–5.5%). Crystals are generally uniform in size (~120 μm), euhedral and lack flow orientation. Clinopyroxene was not found in the Layou deposit. Hornblende is present in the Grand Savanne, Layou and Link Road deposits and consistently displays reaction rims of varying thickness. Ilmenite is rare, but occurs as inclusions in pyroxene crystals. Twinning is common in both plagioclase and pyroxenes. Both zoned and non-zoned plagioclase crystals are present in all units. Although zircon and apatite occur as accessory phases in most units, no zircons were found in the Grand Bay or Grand Savanne deposits.

Plagioclase

Plagioclase compositions in pumices from the major pyroclastic flow units are variable (An_{42} to An_{94}) (Fig. 6C). Although calcic cores are found in Layou and Link Flow 3 plagioclases, all other units show variations of <10 An% in plagioclase profiles. Non-zoned calcic plagioclases (>An_{80}) are found in Goodwill, Geneva, and Link Flow 2 deposits.

Pyroxene

Clinopyroxene compositions are relatively uniform ($En_{36–40}$ and $Wo_{41–44}$; Fig. 6A). All clinopyroxenes found within the Link Road flow units plot within the range $En_{36–39}$. Orthopyroxene compositions in the Goodwill Quarry, Geneva, Grand Bay and Wall House outcrops and Link Road deposits all fall within $En_{51–57}$ (Fig. 6B). Orthopyroxenes in the Layou deposit are less mafic and display a wide range of compositions ($En_{43–53}$). The Londonderry and Grand Savanne deposits both contain more Mg-rich orthopyroxene, > En_{55} (Fig. 6B).

Fe–Ti oxides

The spinel phase (titanomagnetite) is pervasive in all deposits, representing up to 4% of the modal composition, and is generally titaniferous (Usp = 25–35%). Analyses carried out on both free titanomagnetites and titanomagnetite inclusions found in pyroxene reveal no systematic difference. The rhombohedral or ilmenite phase is rare in all deposits, and those analysed were found as inclusions in pyroxene. Titanomagnetites within the Grand Savanne Ignimbrite display evidence of exsolution and are not discussed further. The Goodwill deposits contain titanomagnetites in the compositional range $X_{Usp} = 0.26–0.31$. Although some Grand Bay, Geneva and Wall House crystals overlap with the field of the Goodwill Quarry crystals, the former units are somewhat distinguished by higher X_{Usp} values, lower MgO and Fe_2O_3 (Fig. 7A, B). Titanomagnetites from the Layou pumices are somewhat distinguished by higher Fe_2O_3 and MnO, and lower MgO, compared with crystals in the Goodwill Quarry pumice. Titanomagnetites in pumices from the Londonderry deposit are similarly distinguished by high MgO and Al_2O_3 contents (Fig. 7A, B). In general, titanomagnetite analyses from the Link Flow deposits are similar and plot within the Goodwill Quarry field (Fig. 7D, E). Titanomagnetites from Ash Flows 1 and 2, however, fall outside the Goodwill Quarry field with significantly lower MgO (Fig. 7D) and Al_2O_3 (Fig. 7E).

Fe–Ti oxide temperatures were calculated using the formulation of Ghiorso and Evans (2008). Equilibrium between the phases was chemically determined using the Mn/Mg criteria of Bacon and Hirschmann (1988). The calculated temperature for all units falls between 750 and 900 °C (Fig. 7E). The Goodwill Quarry and Link Road deposits have

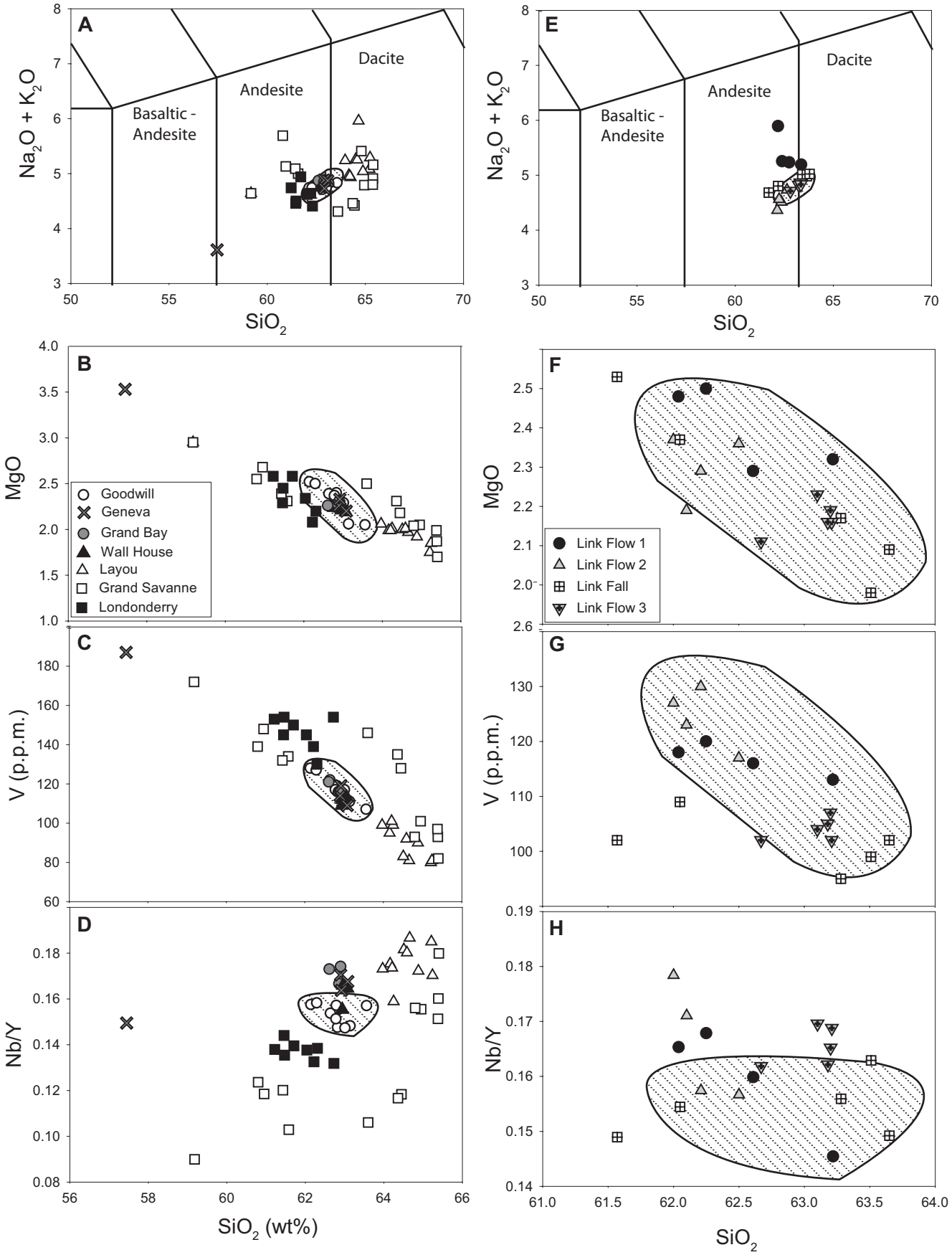

Figure 3. Major and trace element compositions of pumice clasts from Dominica ignimbrite deposits (A–D) and the Link Road pyroclastic flow deposits (E–H). In all cases, the lined field represents the data range of the Goodwill Quarry outcrop. Note the expanded scale on the Link Road plots. TAS diagrams (A and E) are modified from LeBas *et al.* (1992).

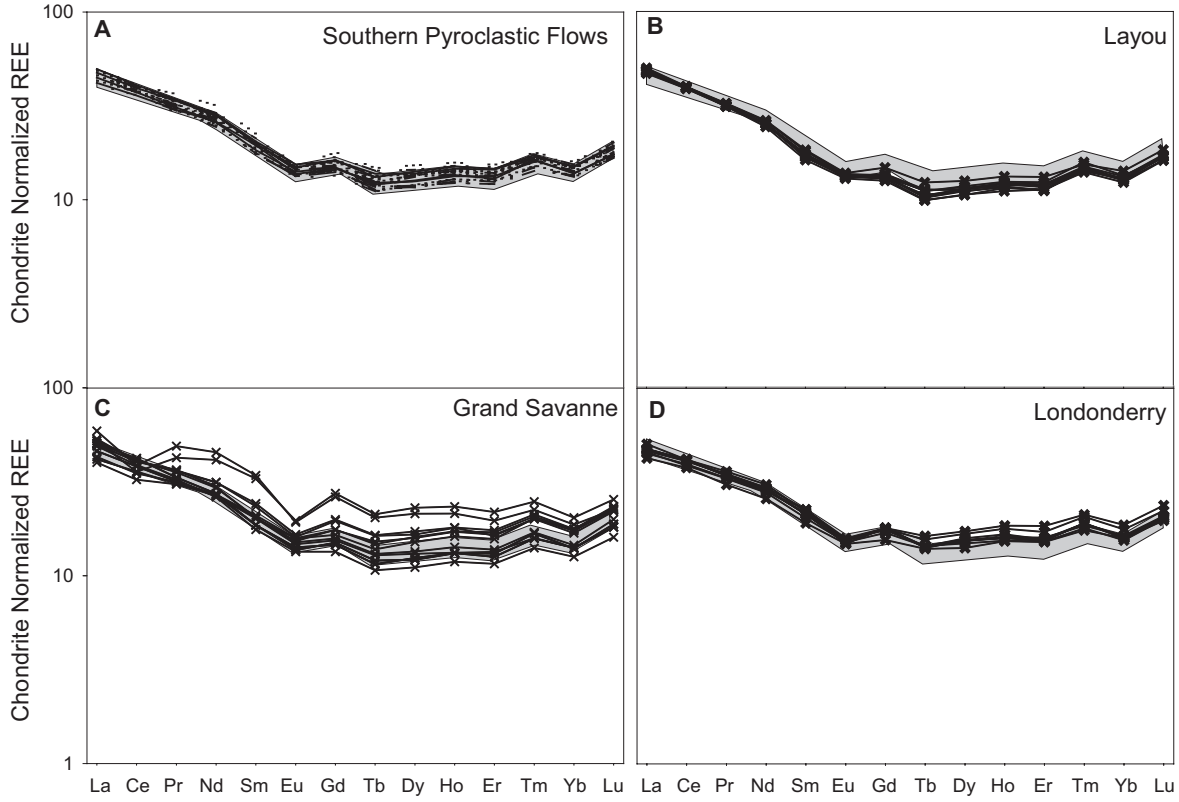

Figure 4. REE compositions of pumice clasts from pumiceous pyroclastic flow deposits. Chondrite values are taken from Sun and McDonough (1989). (A) Pumice clasts from the southern pyroclastic flow deposits (at the Goodwill, Link Road, Grand Bay, Wall House and Geneva outcrops) display a highly limited range. (B) Pumice clasts from Layou, (C) Grand Savanne and (D) Londonderry show more variation. The range of the southern pyroclastic flows is shown in the gray shaded area on each plot.

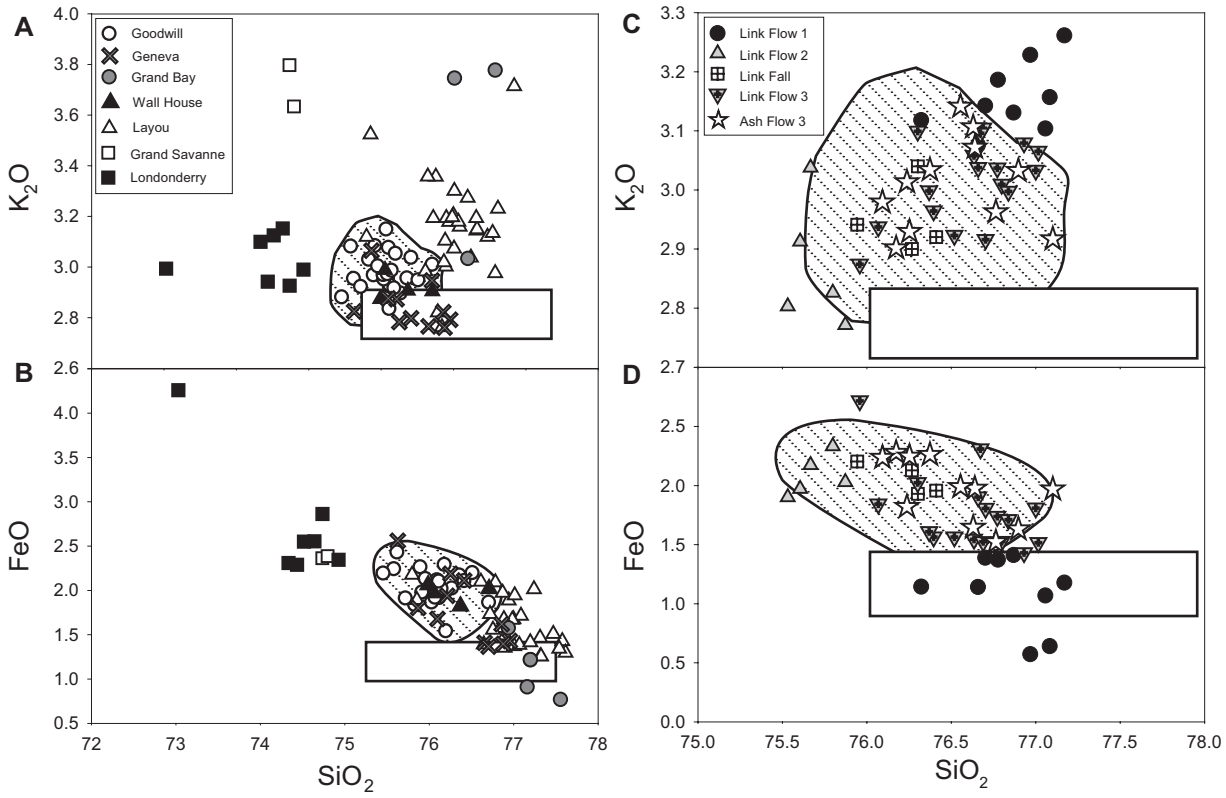

Figure 5. Microprobe analyses of groundmass glass from pumice clasts from all major ignimbrite deposits (A, B) and from Link Road flow and fall deposits (C, D). Note the expanded scale for the Link Road plots. The lined field represents the range of glass data from the Goodwill Quarry deposit (this study). The white box indicates the average compositions of glass (given as oxide major elements $\pm 1\sigma$) for the Roseau Tuff deposit at the Goodwill Quarry as defined by Carey and Sigurdsson (1980).

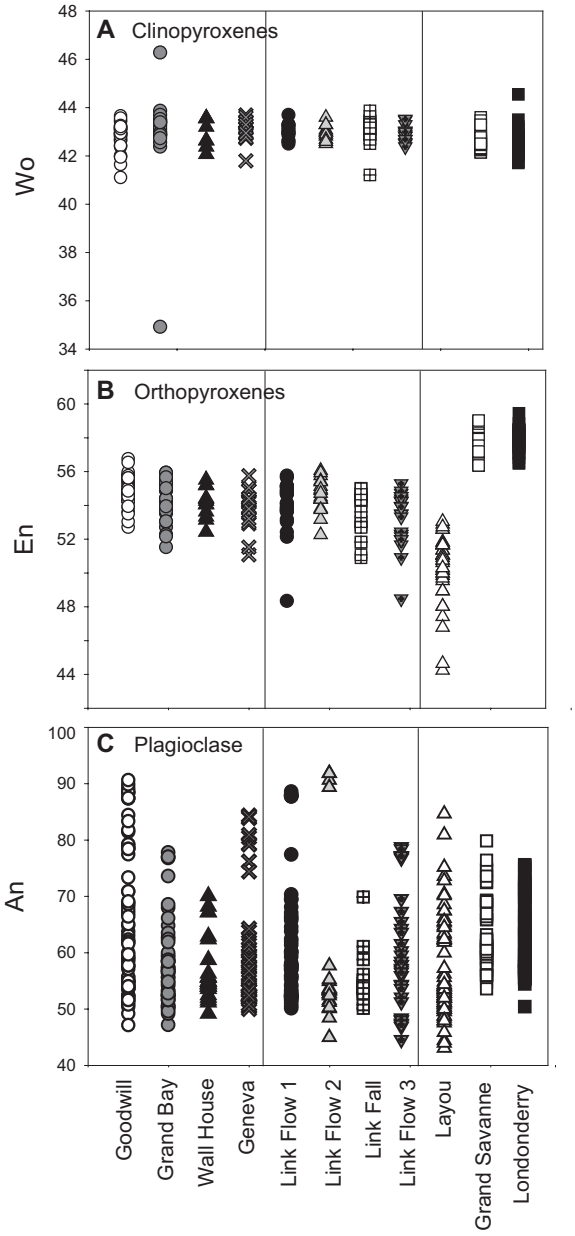

Figure 6. Compositions of clinopyroxenes (A), orthopyroxenes (B) and plagioclase (C) from pumice clasts in the ignimbrite deposits. Note the uniformity of clinopyroxene compositions across the island. Only the southern ignimbrites have uniform orthopyroxene compositions.

a fairly restricted temperature range of 825–875 °C (Fig. 7E). Grand Bay and Geneva deposits have a wider temperature range of ~780–900 °C, whereas temperatures calculated from the Wall House deposit range from 800 to 840 °C. The Layou deposit displays the lowest pre-eruption temperatures (~720–820 °C) and the Londonderry deposits the highest (up to ~900 °C; Fig. 7C). Grand Bay, Wall House and Geneva samples all display lower oxygen fugacities (0.05–0.4 ΔNNO, nickel-nickel oxide oxygen buffer) than those of the Goodwill Quarry deposit (0.35–0.7 ΔNNO) (Fig. 7C). The Layou sample has the lowest fO_2 (down to –0.25 ΔNNO) (Fig. 7C). Although the titanomagnetite chemistry of all the Link units overlap with the Goodwill Quarry field (Fig. 7D, E), oxygen fugacities for the Link Fall and Link Flow 3 deposits (0.1–0.35 ΔNNO) are significantly less than those calculated from the Goodwill Quarry samples (Fig. 7F). Fe–Ti oxide analyses from Ash Flows 2 and 3 also fall outside the Goodwill Quarry range (Fig. 7F).

Amphibole

Amphibole was found in the Layou, Grand Savanne and Link Road deposits (Flows 1–3 and Fall). Although Lindsay *et al.* (2005) and Smith *et al.* (2013) noted rare hornblende in the Roseau Tuff, we found none in the Goodwill Quarry, Grand Bay, Geneva or Wall House outcrops. Amphibole stoichiometry was calculated following Leake *et al.* (1997). All analysed amphiboles have $Ca_A > 1.50$ and $(Na^+K)_A < 0.5$ and are classified as magnesiohornblendes. Amphibole compositions from all units overlap geochemically.

Geochronology

Zircon (U–Th)/He eruption ages

Disequilibrium-corrected zircon (U–Th)/He ages were determined for five deposits: Goodwill Quarry, Link Flow 1, Link Flow 3, Layou and Londonderry. Due to the scarcity of large zircons, averages are based on two to six zircon crystal analyses. Goodness-of-fit values ($Q > 0.1$) indicate high levels of reproducibility between the analysed crystals, and in the absence of any evidence for post-eruptive heating, the (U–Th)/He ages are interpreted as eruption ages (Fig. 8; Table 3). Eruption age averages for individual deposits range from 24 to 80 ka (Fig. 8; Table 3). The oldest eruption age, (~79.7 ± 7.1 ka) is from the Londonderry deposit (Table 3; Fig. 8E). The Layou deposit is the next oldest with an eruption age of ~64.6 ± 4.9 ka (Table 3; Fig. 8E); this is within error of the Goodwill Quarry age of ~61.9 ± 8.0 ka (Table 3; Fig. 8A). Link Flow 1 and Link Flow 3 both have ages significantly younger than the Goodwill Quarry deposit, namely ~34.7 ± 3.1 and ~24.5 ± 2.0 ka, respectively (Table 3; Fig. 8B, C).

Apatite (U–Th)/He eruption ages

Reconnaissance apatite (U–Th)/He ages were determined for three deposits: Goodwill Quarry, Grand Bay and Layou. Although apatites were also found in the Londonderry and Grand Savanne units, they were significantly fractured and altered, and yielded unrealistic ages. Apatites from the Goodwill Quarry deposit generated an age of 50.8 ± 3.3 ka (Table 4; Fig. 9), which overlaps within error of the associated zircon age for this deposit. The Grand Bay and Layou deposits yielded ages of 62.6 ± 4.0 and 79.7 ± 4.8 ka, respectively (Table 4; Fig. 9).

Discussion

Comparison of (U–Th)/He ages with published ^{14}C ages

As many of the previously published ^{14}C ages associated with the pyroclastic flow deposits on Dominica are minimum ages (indicated by the '>' symbol before the age) (Table 2) and little information on the types of materials used is available, it is difficult to assess their quality or geologic context. The new (U–Th)/He ages therefore provide important constraints on the chronological history of pyroclastic activity on the island. Due to the low uranium content of zircon (<100 p.p.m.) and apatite (<5 p.p.m.) and the young age of the deposits, analytical precision is generally lower than in comparable studies (e.g. Schmitt *et al.*, 2010a).

Zircon and apatite (U–Th)/He ages from the Goodwill Quarry outcrop (Location 1; Fig. 1) overlap within error, placing this eruption at ~55 ka (Fig. 10). Although previously determined ^{14}C ages indicate that the Roseau Tuff eruption as defined by Carey and Sigurdsson (1980) occurred at ~30k cal

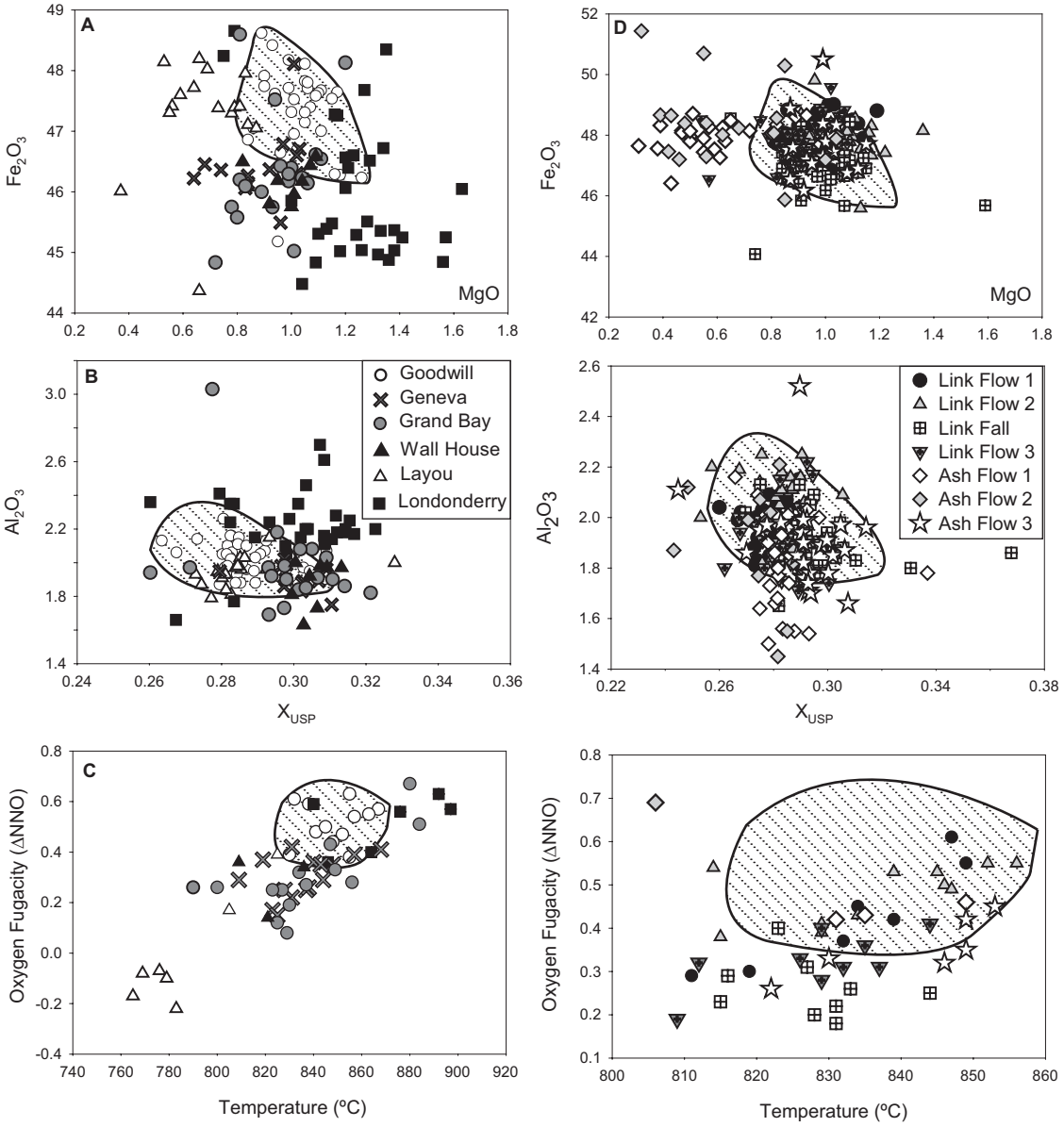

Figure 7. Magnetite chemistry of major pyroclastic deposits (A, B) and Link Road deposits (D, E), and calculated temperatures and oxygen fugacities (Ghiorso and Evans, 2008) for major pyroclastic flows (C) and Link Road deposits (F). The lined field represents the range of magnetite data from the Goodwill Quarry deposit.

a BP (Table 2; Fig. 10), the stratigraphy of volcanic deposits in the Roseau Valley is poorly constrained and the relationship of dated units to mapped units is uncertain (Smith *et al.*, 2013). Field mapping by Sigurdsson (1972) indicates that the oldest Roseau eruption, denoted Unit I, occurred at >45k cal a BP (Table 2). This agrees with our estimated age of ~55 ka. Pyroclastic flow deposits along the Link Road Outcrop (Location 2; Fig. 1) yielded stratigraphically consistent (U−Th)/He ages of ~34.7 ± 3.1 and ~24.5 ± 2.0 ka (Table 3; Fig. 8B, C). The older age (from Link Flow 1) is within error of ^{14}C ages for Unit II of the Roseau Sequence (Fig. 10). The younger age (from the stratigraphically higher Link Flow 3) is ~5 ka younger than any previous ^{14}C ages for the Roseau deposits (Fig. 10; Table 2). Although it is unclear whether this unit is related to Unit III of the Roseau Tuff or represents a later stage in activity, we suggest that it has never been dated before. Our new (U−Th)/He ages extend the known age range of the Roseau Sequence from 30–45k cal a BP to 24–61 ka.

Apatite from the Grand Bay Beach deposit (Location 16; Fig. 1) yielded a (U−Th)/He age of ~62 ka. Although ^{14}C ages from distal outcrops at Stowe, Fond. St. Jean and Wall House indicate that this eruption occurred at ~35k cal a BP (Fig. 10), Smith *et al.* (2013) suggest that these deposits are unlikely to be related to the Grand Bay Beach outcrop based on lithologic constraints.

Zircon and apatite (U−Th)/He ages for the Layou deposit overlap within 2σ uncertainties (Fig. 10), but the spread in apatite ages (Fig. 9) indicates the presence of U-rich inclusions in a few of the studied aliquots. We thus consider the zircon (U−Th)/He age of ~64.6 ± 4.9 ka ($Q = 0.84$; Fig. 8) to be more reliable because it closely matches the independently determined U−Th zircon crystallization age. These ages are consistent with the ^{14}C minimum age of >40k cal a BP (Wadge, 1989) (Fig. 10).

Correlation of pyroclastic flow deposits on Dominica

Northern pyroclastic flow deposits

Based on whole rock (Fig. 3), glass (Fig. 5), Fe−Ti oxide (Fig. 7) and orthopyroxene (Fig. 6B) analyses, we suggest that

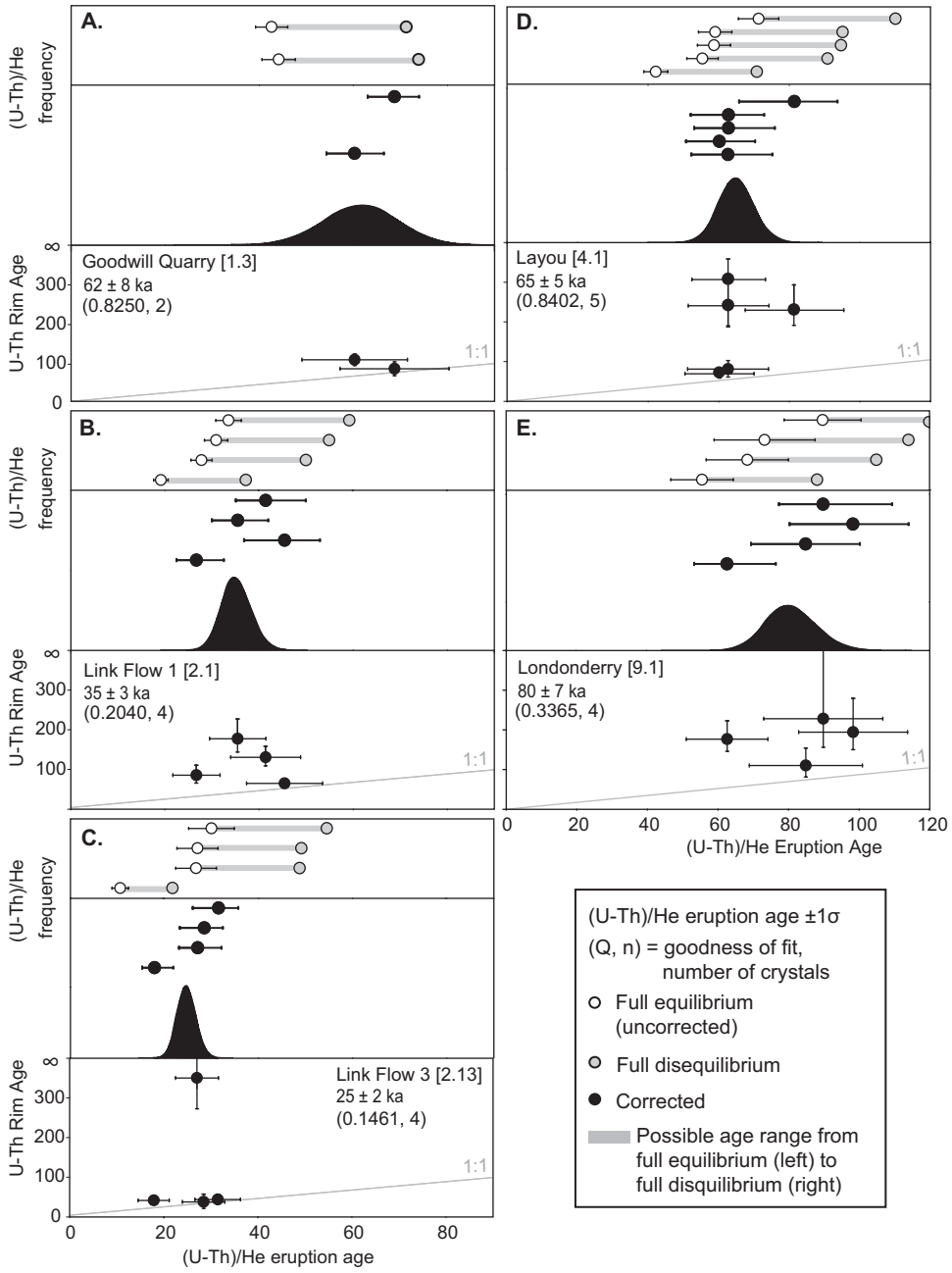

Figure 8. Combined U−Th and (U−Th)/He zircon ages. From top to bottom, panels show uncorrected and full disequilibrium ages, disequilibrium-corrected ages, Gaussian fits of the modeled eruption ages, and a comparison between U−Th crystallization ages and the calculated (U−Th)/He eruption age. Errors shown are 1 SD.

the northern ignimbrites, sampled at the Grand Savanne and Londonderry outcrops, are different from their southern counterparts. In general, these northern deposits can be distinguished by less evolved glass compositions (73–75 wt% SiO_2) and more mafic orthopyroxene compositions (En > 56) (Fig. 6B). In addition, (U−Th)/He ages suggest that the Londonderry deposit is ∼20 ka older than the oldest of the southern deposits (Fig. 10). While we did not map the deposits to their source locations, we agree with Sparks *et al.* (1980) and Smith *et al.* (2013) that both deposits are probably sourced from Diablotins volcano given topographic constraints. As these two deposits can be distinguished by glass and whole rock chemistry (Fig. 5), we agree with Smith *et al.* (2013) that they probably represent two separate eruptions. Smith *et al.* (2013) further suggest that the Point Ronde flow deposit (not studied here) represents yet another separate eruption from Diablotins.

Southern pyroclastic flow deposits

Due to their uniform geochemistry, correlation of pyroclastic flow deposits in the southern half of Dominica is difficult and the deposits have been variously correlated as part of the Roseau Tuff (Carey and Sigurdsson, 1980; Whitham, 1989; Smith *et al.*, 2013), the Grand Bay Ignimbrite (Lindsay *et al.*, 2003) and the Layou Ignimbrite (Demange *et al.*, 1985; Smith *et al.*, 2013). Based on new data, we suggest that the southern ignimbrites can be subdivided into the Roseau Sequence and the Layou Ignimbrite. The Roseau Sequence includes ignimbrites at the Goodwill Quarry, Grand Bay, Geneva, Wall House and Link Road outcrops, which cannot be distinguished from one another by whole rock or trace element geochemistry (Fig. 3A–D). Although the presence of amphibole in the Link Road Units may be a distinguishing feature, its apparent absence in other deposits may simply reflect its scarcity. Fe−Ti oxide compositions of all these units show slight differences (Fig. 7). However, most samples overlap to some degree, making it impossible to accurately separate units based on titanomagnetite chemistry alone. The exception is titanomagnetite analyses from Ash Flows 1 and 2, which have significantly less MgO (Fig. 7). This indicates that these ashy pyroclastic flows may not be related the Roseau Sequence eruptions.

Table 3. U−Th and (U−Th)/He zircon results for pumice clasts from ignimbrites on Dominica. Eruption ages are based on MCHeCalc calculations producing best fit estimates of crystallization age.

Helium aliquot	$^{238}U/^{232}Th$	$^{230}Th/^{232}Th$	(U−Th) age (ka ± SD)	U (p.p.m)	Th (p.p.m)	D230	Ft	Equilibrium (U−Th)/He age (ka ± SD)	Full dis-equilibrium	Corrected (U−Th)/He age (ka ± SD)
TH-DM-4.1. Layou. 15°23.859N, 61°25.607W, (U−Th)/He age 64.6 ka (+5.1–4.8 ka), $n=5$, goodness-of-fit = 0.8402.										
zLay4-1	8.30 ± 0.32	7.84 ± 0.81	307 ± 118	46.6	17.9	0.115	0.84	59.0 ± 9.4	95.1	62.9 ± 10
zLay4-2	6.66 ± 0.13	6.01 ± 0.40	241 ± 116	54.8	21.2	0.116	0.84	58.7 ± 9.4	94.7	63.5 ± 12.4
zLay4-3	5.90 ± 0.08	5.28 ± 0.26	229 ± 62	77.3	32.4	0.126	0.81	71.3 ± 11.4	110	81.5 ± 11.7
z4-2-1	6.59 ± 0.06	3.55 ± 0.30	81.2 ± 18.3	86.4	38.1	0.132	0.81	42.2 ± 6.7	70.9	62.7 ± 12.4
z4-2-2	6.74 ± 0.05	3.95 ± 0.47	69.1 ± 10.7	37.2	13.5	0.109	0.88	55.4 ± 8.9	90.9	84.3 ± 20
TH-DM-9.1. Londonderry. 15°33.614N, 61°17.832W, (U−Th)/He age 79.7 ka (+7.9–6.3 ka), $n=4$, goodness-of-fit = 0.3365.										
zLon9-1	6.83 ± 0.14	5.64 ± 0.33	177 ± 39	66.6	31.8	0.143	0.82	55.2 ± 8.8	87.8	63.8 ± 13.3
zLon9-2	6.52 ± 0.16	5.56 ± 0.43	194 ± 71	40.8	14.7	0.108	0.87	72.9 ± 11.7	114	84.8 ± 16.5
zLon9-3	7.75 ± 0.14	6.89 ± 0.65	228 ± 163	89.0	42.9	0.145	0.78	89.4 ± 14.3	131	95.2 ± 19.2
zLon9-10	7.74 ± 0.12	5.24 ± 0.71	110 ± 31	88.2	41.9	0.142	0.82	68.1 ± 10.9	105	93.2 ± 16.4
TH-DM-1.3. Roseau Tuff. (U−Th)/He age 61.9 ka (+7.6–8.2 ka), $n=2$, goodness-of-fit = 0.8250.										
z2-1-1	6.42 ± 0.08	3.88 ± 0.51	85.4 ± 22.1	33.2	11.9	0.107	0.86	19.3 ± 3.1	37.4	26.7 ± 3.9
z2-1-2	8.84 ± 0.05	4.44 ± 0.18	65.0 ± 4.6	63.7	27.0	0.127	0.87	27.9 ± 4.5	50.1	45.0 ± 4.0
z2-1-4	6.39 ± 0.03	4.71 ± 0.37	130 ± 24	51.9	20.9	0.120	0.82	33.7 ± 5.4	59.4	41.9 ± 5.0
z2-1-5	8.07 ± 0.05	6.65 ± 0.51	177 ± 40	41.0	17.3	0.126	0.85	31.1 ± 5.0	55.1	35.7 ± 3.4
TH-DM-2.13. Link flow. 3 15°18.256N, 61°22.465W, U−Th)/He age 24.5 ka (+2.1–2.0 ka), $n=4$, goodness-of-fit = 0.1461.										
z2-13-1	7.30 ± 0.04	2.91 ± 0.33	41.6 ± 8.2	34.2	13.7	0.120	0.87	10.9 ± 1.7	22.0	17.9 ± 4.0
z2-13-3	9.36 ± 0.05	3.68 ± 0.61	43.8 ± 11.8*	30.3	11.3	0.112	0.90	30.3 ± 4.8	54.8	S.E.
z2-13-5	1.00 ± 0.02	1.00 ± 0.46	S.E.	56.1	22.8	0.122	0.87	27.0 ± 4.3	49.0	S.E.
z2-13-6	4.44 ± 0.05	1.92 ± 0.41	37.9 ± 17.8*	52.0	21.4	0.123	0.83	27.3 ± 4.4	49.4	S.E.

*U−Th age was changed to secular equilibrium. S.E. refers to secular equilibrium U-Th values. D230 = [(Th/U)zircon/(Th/U)whole-rock] × (230Th)/(238U)whole-rock. Ft = Percentage of He retained in the crystal based on the alpha-ejection correction.

Table 4. (U−Th)/He apatite results for pumice clasts from pyroclastic flow deposits on Dominica. Eruption ages are based on the average age of all aliquots.

Sample	(U−Th)/He age (ka ± SD)	U (p.p.m.)	Th (p.p.m.)	^{147}Sm (p.p.m.)	[U]e	Ft
TH-DM-1.3. Goodwill Quarry. (U−Th)/He age 50.8 ka (± 3.3 ka), $n=11$.						
aRose1-1	55.0 ± 4.4	2.5	6.7	27.0	4.2	0.74
aRose1-3	50.3 ± 4.0	3.3	8.5	36.9	5.4	0.69
aRose1-4	57.9 ± 4.6	3.7	9.6	37.0	6.1	0.71
a1-3-2	49.1 ± 2.9	2.6	7.0	32.4	4.4	0.71
a1-3–4	50.8 ± 3.0	2.9	7.7	33.6	4.9	0.70
a1-3–5	54.1 ± 3.2	3.0	7.9	29.9	5.0	0.73
a1-3–6	48.3 ± 2.9	2.6	7.1	30.9	4.4	0.72
a1-3–7	43.6 ± 2.6	2.9	7.7	33.1	4.9	0.72
a1-3–8	50.2 ± 3.0	3.1	8.2	36.9	5.2	0.72
a1-3–9	59.3 ± 3.6	3.0	8.2	33.9	5.1	0.72
a1-3–10	39.9 ± 2.4	2.5	6.7	29.9	4.2	0.77
TH-DM-16.2. Grand Bay. (U−Th)/He age 62.6 ka (± 4.0 ka), $n=11$.						
aGrand16-1	60.8 ± 4.9	4.0	11.1	34.3	6.8	0.72
aGrand16-4	59.7 ± 4.8	3.3	8.5	37.5	5.4	0.65
a16-2-1	77.4 ± 4.6	2.9	8.3	35.5	5.0	0.71
a16-2-2	56.9 ± 3.4	3.2	8.6	36.2	5.3	0.76
a16-2-3	50.3 ± 3.0	2.0	5.3	26.1	3.4	0.73
a16-2-4	77.3 ± 4.6	2.8	7.9	35.8	4.8	0.73
a16-2-5	66.4 ± 4.0	2.6	7.4	36.0	4.5	0.69
a16-2-6	87.1 ± 5.2	2.7	7.4	31.0	4.6	0.74
a16-2-7	47.2 ± 2.8	2.8	7.7	35.1	4.8	0.76
a16-2-8	50.7 ± 3.0	3.3	9.0	38.9	5.6	0.74
a16-2-9	54.7 ± 3.3	2.6	7.1	31.8	4.4	0.71
TH-DM-4.1. Layou. (U−Th)/He age 79.7 ka (± 4.8 ka), $n=8$.						
a4-2-1	81.4 ± 4.9	4.3	10.7	31.0	7.0	0.71
a4-2-2	94.2 ± 5.7	4.1	10.0	29.1	6.5	0.70
a4-2-3	76.2 ± 4.6	4.0	10.1	27.4	6.4	0.69
a4-2-4	88.5 ± 5.3	3.1	9.6	26.8	5.5	0.69
a4-2-5	74.0 ± 4.4	3.9	9.9	25.5	6.3	0.73
a4-2-6	67.0 ± 4.0	3.2	7.7	20.9	5.0	0.73
a4-2-7	78.2 ± 4.7	4.5	11.0	28.5	7.2	0.71
a4-2-8	78.1 ± 4.7	4.5	10.8	25.5	7.1	0.74

[U]e (effective uranium concentration) = U + 0.235Th. Ft = Percentage of He retained in the crystal based on the alpha-ejection correction.

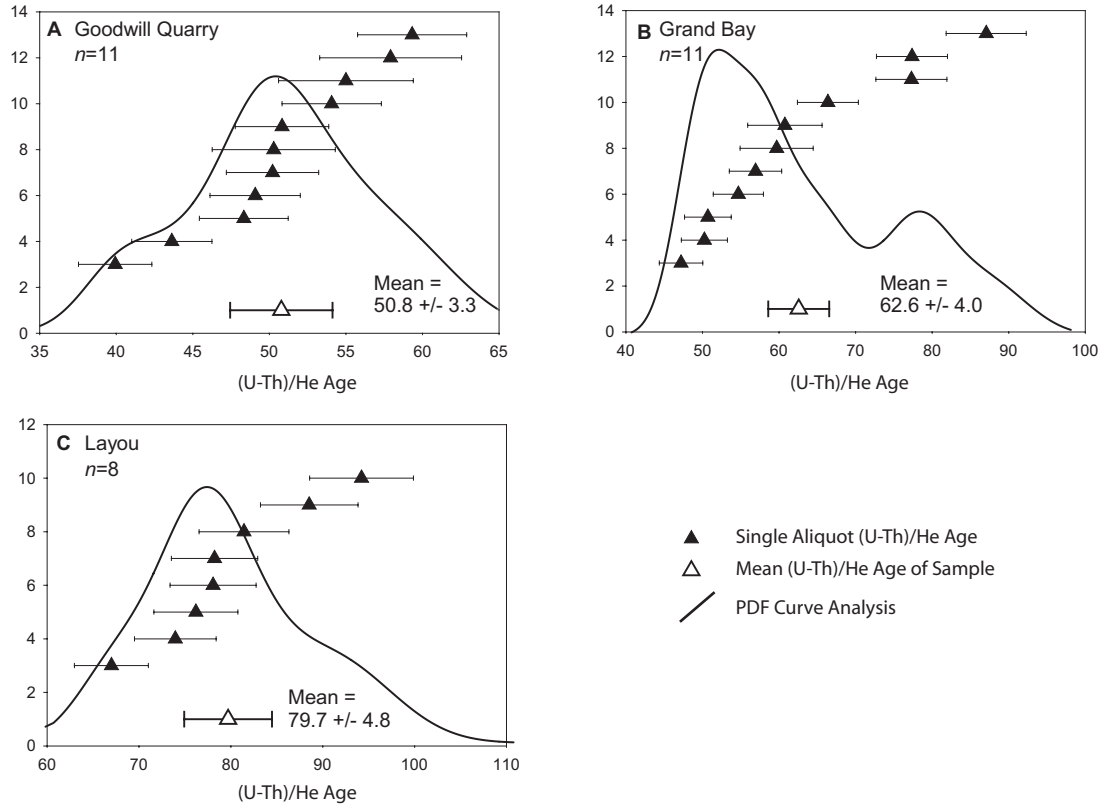

Figure 9. (U–Th)/He apatite ages for the Goodwill Quarry (A), Grand Bay (B) and Layou (C) deposits. Plots show all aliquot ages and mean eruption age for each sample. Errors shown are 1 SD; vertical axes show numbers of analyses.

The distinct eruption ages of the southern deposits (~24–61 ka; Tables 3 and 4), when combined with the presence of three soil horizons dividing the sequence at Link Road (Fig. 2), suggests that despite their geochemical homogeneity, they cannot be the result of a single, large eruption. Indeed, their ages and the presence of paleosols point to the occurrence of at least six separate explosive eruptions of varying sizes. This finding agrees with that of Smith *et al.* (2013), who proposed that the Roseau Tuff deposits represent up to seven separate eruptions. Due to their close geochemical similarity (Table 5), we suggest that all six eruptions are sourced from the same center. Although we cannot determine

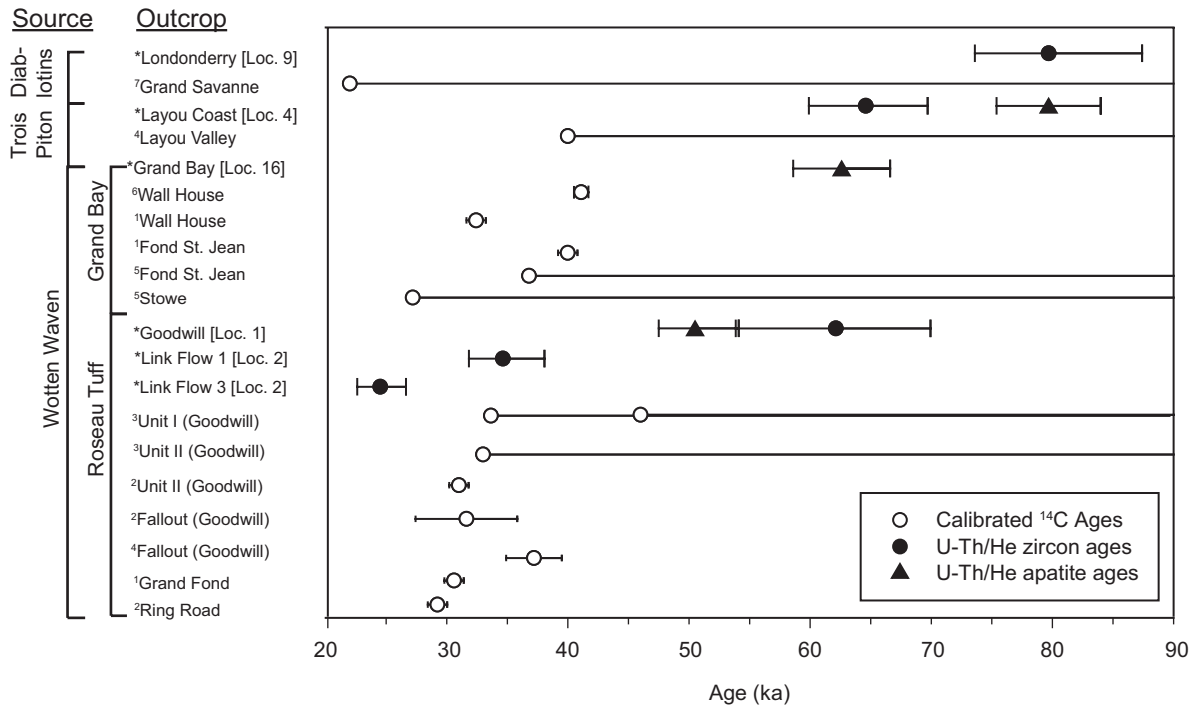

Figure 10. Comparison of new (U–Th)/He ages (*) with calibrated ^{14}C ages from previous work detailed in Table 2 (references are shown as superscripts – see Table 2 caption for reference list). Error bars extending to the right of the plot indicate minimum ages. All errors shown are 1 SD. Location numbers refer to sample locations shown on Fig. 1.

Table 5. Geochemical characteristics of pumice clasts from the Roseau sequence compared with the island-wide range for pumice clasts found within all ignimbrites on Dominica.

	Roseau sequence	Island wide
Whole rock (pumice clasts)		
SiO_2 (wt%)	62–64	57–66
Al_2O_3 (wt%)	16.5–17.5	15.8–18.9
FeO (wt%)	5.5–7.3	5.2–8.9
K_2O (wt%)	1.4–1.8	1.4–2.0
Groundmass glass		
SiO_2 (wt%)	75.5–77	73.0–77.9
Al_2O_3 (wt%)	12–13	11.9–13.2
FeO (wt%)	1–2.2	0.7–3.0
K_2O (wt%)	2.6–3.2	2.7–3.8
Magnetite		
average X_{USP}	0.26–0.31	0.26–0.33
Clinopyroxene		
Wo range	41–44	41–44
Orthopyroxene		
En range	48–57	43–61
Plagioclase		
An range	45–95	40–95

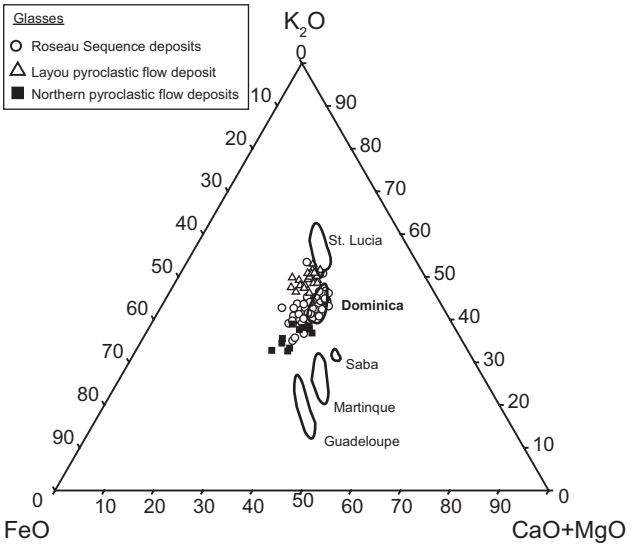

Figure 11. Plot showing fields from Sigurdsson and Carey (1981) representing the range of glass compositions for individual islands in the Lesser Antilles (based on a composite of analyses from material collected from multiple eruptive units on each island). Dominica glass analyses from this study are plotted on this diagram to illustrate that the previously determined fields probably represent limited ranges based on small sample sets.

the individual volume of these eruptions or the total volume of the Roseau sequence, we propose that these eruptions are relatively small. The Layou pyroclastic flow deposit has strikingly different whole rock, glass and mineral chemistry from the Roseau sequence deposits and is thus unrelated. Based on topographic constraints, we suggest that this deposit is sourced from Trois Piton (Table 4), which agrees with previous assessments (Sigurdsson, 1972; Smith *et al.*, 2013).

Implications for tephrostratigraphy

The 58 km^3 (unconsolidated) volume of the Roseau Tuff was based on correlation of tephra layers and pyroclastic flow deposits in deep sea cores to a pyroclastic flow unit at the Goodwill Quarry (Carey and Sigurdsson, 1980). Based on the geochemistry alone, the pyroclastic deposits on southern Dominica are almost indistinguishable and could be erroneously considered the result of a single eruption. Our new (U−Th)/He geochronology, together with the presence of three paleosols between the flow units in the Link Road deposit (Fig. 2), indicates that the southern pyroclastic flows were deposited by at least six separate eruptions between 24 and 61 ka. Because the geochemical and petrographic homogeneity of these deposits makes it difficult to correlate closely spaced onshore deposits on Dominica, it is unlikely that correlations made to specific tephra layers in deep sea cores are reliable. We agree with Smith *et al.* (2013) that the Roseau Tuff 'eruption' as defined by Carey and Sigurdsson (1980) is probably a series of smaller eruptions, each producing some material preserved offshore. According to Smith *et al.* (2013), the cores studied by Carey and Sigurdsson (1980) all show internal stratification and interbedding of pyroclastic flow and pyroclastic turbidite deposits that could reflect multiple eruptions. The cores also show evidence of extensive bioturbation, which can obliterate ash-fall layers <1 cm in thickness (Sigurdsson and Carey, 1981). It is further noted that during periods of slow sedimentation, amalgamation of tephra layers can occur because intervening sedimentation may be insignificant. Although it may be possible to correlate tephra layers in deep sea cores from the Lesser Antilles to individual volcanic islands (given that eruptive deposits on each island display common geochemical characteristics; see Sigurdsson and Carey, 1981) or even to individual centers on those islands (Fig. 11), it is presently premature, at least on Dominica, to correlate them with individual onshore eruptive units. Furthermore, our results indicate that the compositional range of glass from Dominica deposits previously used for correlation (Sigurdsson and Carey, 1981) does not adequately represent the actual glass compositional range of the onshore deposits (Fig. 11).

Conclusions

1. Pyroclastic flow deposits from several major eruptions on southern Dominica are stratigraphically poorly constrained, and display similar whole rock, glass and mineral chemistry. This makes them difficult to distinguish for correlation purposes.
2. New (U−Th)/He ages suggest that pyroclastic flow deposits on the island span a wider time range than previously thought. Significant explosive eruptions occurred between 24 and 80 ka.
3. Our work suggests that (U−Th)/He geochronology is a valuable method for dating Quaternary volcanic rocks that can fill the chronological gap in regions where ^{14}C and K−Ar or Ar/Ar methods are not applicable.
4. The Roseau Tuff eruption defined by Carey and Sigurdsson (1980) is probably a series of smaller eruptions with similar geochemical and petrographic characteristics. This sequence represents at least six eruptions that occurred between 24 and 61 ka. The Grand Bay Ignimbrite, which was previously mapped as resulting from a separate eruption, is now considered part of this sequence.
5. Although glass chemistry from tephra in deep sea cores in the Lesser Antilles can be used to correlate to individual islands and perhaps even to individual volcanic centers on

those islands, correlations to single eruptive events are tenuous at best, especially for southern Dominica.

Supporting Information

Additional supporting information can be found in the online version of this article:

Table S1: The full suite of whole rock, glass and mineral chemistry data used in this project.
Table S2: Representative whole rock major and trace element analyses for pumice clasts from each outcrop.
Table S3: Representative groundmass glass shards from pumice clasts found within Dominica ignimbrites.

Acknowledgements. This study was funded by the University of Auckland Doctoral Fellowship scheme, an internal University of Auckland PBRF grant, and a New Zealand GNS Science contract. J.M. L. gratefully acknowledges support from the New Zealand Earthquake Commission. The ion microprobe facility at UCLA is partly supported by a grant from the Instrumentation and Facilities Program, Division of Earth Sciences, National Science Foundation. Thanks to Ritchie Sims, John Wilmshurst, Roman Kislitsyn, Charlotte Allan and Andres Arcila Rivera for technical support.

Abbreviations. MSWD, mean square weighted deviation; NNO, nickel-nickel oxide oxygen buffer; REE, rare earth element; XRF, X-ray fluorescence

References

Bacon CR, Hirschmann MM. 1988. Mg/Mn partitioning as a test for equilibrium between coexisting Fe–Ti oxides. *American Mineralogist* **73**: 57–61.

Biswas S, Coutand I, Grujic D, *et al*. 2007. Exhumation and uplift of the Shillong plateau and its influence on the eastern Himalayas: new constraints from apatite and zircon (U–Th-[Sm])/He and apatite fission track analyses. *Tectonics* **26**: TC6013.

Brendryen J, Haflidason H, Sejrup HP. 2010. Norwegian Sea tephrostratigraphy of marine isotope stages 4 and 5: prospects and problems for tephrochronology in the North Atlantic region. *Quaternary Science Reviews* **29**: 847–864.

Carey SN, Sigurdsson H. 1980. The Roseau Ash: deep-sea tephra deposits from a major eruption on Dominica, Lesser Antilles arc. *Journal of Volcanology and Geothermal Research* **7**: 67–86.

Danišík M, Shane P, Schmitt AK, *et al*. 2012. Re-anchoring the Late Pleistocene tephrochronology of New Zealand based on concordant radiocarbon ages and combined $^{238}U/^{230}Th$ disequilibrium and (U–Th)/He zircon ages. *Earth and Planetary Sciences Letters* **349–350**: 240–250.

Demange J, Leborne H, Traineau H, *et al*. 1985. *Histoire Volcano-Structurale De La Region Sud de la Dominique*. Institute Mixte Recherches Geothermiques: Orleans, France.

Farley KA. 2000. Helium diffusion from apatite: general behavior as illustrated by Durango fluorapatite. *Journal of Geophysical Research: Solid Earth* **105**: 2903–2914.

Farley KA. 2002. (U–Th)/He dating: techniques, calibrations, and applications. *Reviews in Mineralogy and Geochemistry* **47**: 819–844.

Farley KA, Kohn BP, Pillans B. 2002. The effects of secular disequilibrium on (U–Th)/He systematics and dating of Quaternary volcanic zircon and apatite. *Earth and Planetary Science Letters* **201**: 117–125.

Froggatt PC, Gosson GJ. 1982. *Techniques for the Preparation of Tephra Samples for Mineral and Chemical Analysis and Radiometric Dating*. Victoria University of Wellington: 23–24.

Ghiorso MS, Evans BW. 2008. Thermodynamics of rhombohedral oxide solid solutions and a revision of the Fe–Ti two-oxide geothermometer and oxygen-barometer. *American Journal of Science* **308**: 957–1039.

Hildreth W, Mahood G. 1985. Correlation of ash-flow tuffs. *Geological Society of America Bulletin* **96**: 968–974.

Leake BE, Woolley AR, Arps CES, *et al*. 1997. Nomenclature of amphiboles: report of the Subcommittee on amphiboles of the International Mineralogical Association: Commission on New Minerals and Mineral Names. *American Mineralogist* **82**: 1019–1037.

LeBas MJ, Maitre RW, Woolley AR. 1992. The construction of the total alkali-silica chemical classification of volcanic rocks. *Mineralogy and Petrology* **46**: 1–22.

Lindsay J, Robertson R, Shepherd B, *et al*. editors. 2005. *Volcanic Hazard Atlas of the Lesser Antilles*. Seismic Research Centre, Trinidad and IAVCEI: University of the West Indies.

Lindsay J, Stasiuk M, Shepherd J. 2003. Geological history and potential hazards of the late-Pleistocene to Recent Plat Pays volcanic complex, Dominica, Lesser Antilles. *Bulletin of Volcanology* **65**: 201–220.

Lowe DJ. 2011. Tephrochronology and its application: a review. *Quaternary Geochronology* **6**: 107–153.

Norrish K, Chappell BW. 1977. *X-ray Fluorescence Spectrometry*. Academic Press: London.

Paces JB, Miller JD. 1993. Precise U–Pb ages of Duluth Complex and related mafic intrusions, northeastern Minnesota: geochronological insights to physical, petrogenetic, paleomagnetic, and tectonomagmatic processes associated with the 1.1 Ga Midcontinent Rift System. *Journal of Geophysical Research: Solid Earth* **98**(B8): 13 997–14 013.

Press WH, Teukolsky SA, Vetterling WT, *et al*. 1992. *Numerical Recipes in C*. 2nd edn. Cambridge University Press: Cambridge.

Sarna-Wojcicki A. 2000. *Tephrochronology, Quaternary Geochronology*. American Geophysical Union: Washington, DC.

Schmitt AK, Stockli DF, Hausback BP. 2006. Eruption and magma crystallization ages of Las Tres Vírgenes (Baja California) constrained by combined $^{230}Th/^{238}U$ and (U–Th)/He dating of zircon. *Journal of Volcanology and Geothermal Research* **158**: 281–295.

Schmitt AK, Stockli DF, Lindsay JM, *et al*. 2010a. Episodic growth and homogenization of plutonic roots in arc volcanoes from combined U–Th and (U–Th)/He zircon dating. *Earth and Planetary Science Letters* **295**: 91–103.

Schmitt AK, Stockli DF, Niedermann S, *et al*. 2010b. Eruption ages of Las Tres Vírgenes volcano (Baja California): a tale of two helium isotopes. *Quaternary Geochronology* **5**: 503–511.

Shane P, Smith I. 2000. Geochemical fingerprinting of basaltic tephra deposits in the Auckland Volcanic Field. *New Zealand Journal of Geology and Geophysics* **43**: 569–577.

Sigurdsson H. 1972. Partly-welded pyroclast flow deposits in Dominica, Lesser Antilles. *Bulletin of Volcanology* **36**: 148–163.

Sigurdsson H, Carey S. 1981. Marine tephrochronology and Quaternary explosive volcanism in the Lesser Antilles arc. In *Tephra Studies*, Self S, Sparks RSJ (eds). Springer: Dordrecht. NATO Advanced Study Institutes Series; 255–280.

Sigurdsson H, Carey SN. 1991. *Caribbean Volcanoes: A Field Guide*. Geological Association of Canada, Toronto '91 Organizing Committee: Sudbury, Ontario, Canada.

Smith AL, Roobol MJ, Mattioli GS, *et al*. 2013. *The Volcanic Geology of the Mid-Arc Island of Dominica, Lesser Antilles: the Surface Expression of an Island-Arc Batholith*. Geological Society of America: Boulder, CO.

Sparks RSJ, Sigurdsson H, Carey SN. 1980. The entrance of pyroclastic flows into the sea I. oceanographic and geologic evidence from Dominica, Lesser Antilles. *Journal of Volcanology and Geothermal Research* **7**: 87–96.

Sun S, McDonough WF. 1989. Chemical and isotopic systematics of oceanic basalts: implications for mantle composition and processes. *Geological Society, London, Special Publications* **42**: 313–345.

Wadge G. 1989. *A Preliminary Analysis of Volcanic Hazards in Dominica*. Seismic Research Unit: St. Augustine, Trinidad.

Wadge G, Shepherd JB. 1984. Segmentation of the Lesser Antilles subduction zone. *Earth and Planetary Science Letters* **71**: 297–304.

Westgate JA, Gorton MP. 1981. Correlation techniques in tephra studies. In *Tephra Studies*, Self S, Sparks RSJ (eds). Springer: Dordrecht. NATO Advanced Study Institutes Series; 73–94.

Whitham AG. 1989. The behaviour of subaerially produced pyroclastic flows in a subaqueous environment: evidence from the Roseau eruption, Dominica, West Indies. *Marine Geology* **86**: 27–40.